Injectivity of Multiple Gas and Liquid Slugs in SAG Foam EOR: A CT Scan Study

Gong, Jiakun; Vincent-Bonnieu, S.; Kamarul Bahrim, R. Z.; Che Mamat, C.A.N.B.; Tewari, R.D.; Mahamad Amir, M.I.; Groenenboom, J.; Farajzadeh, Rouhi; Rossen, Bill

DOI
10.3997/2214-4609.201900107

Publication date
2019

Document Version
Final published version

Published in
IOR 2019 – 20th European Symposium on Improved Oil Recovery

IOR 2019
20TH EUROPEAN SYMPOSIUM ON IMPROVED OIL RECOVERY

EAGE

Tu A 09

Injectivity of Multiple Gas and Liquid Slugs in SAG Foam EOR: A CT Scan Study

J. Gong[1]*, S. Vincent-Bonnieu[2], R.Z. Kamarul Bahrim[3], C.A.N.B. Che Mamat[3], R.D. Tewari[3], M.I. Mahamad Amir[3], J. Groenenboom[2], R. Farajzadeh[1,2], W. Rossen[1]

[1]Delft University of Technology; [2]Shell Global Solutions International B.V.; [3]PETRONAS

Summary

Surfactant-alternating-gas (SAG) is often the injection method for foam enhanced oil recovery (EOR) in order to improve injectivity. However, liquid injectivity can be very poor once foam is created in the near-wellbore region. In a previous study, we reported core-flood experiments on liquid injectivity after foam flooding and liquid injectivity after a period of gas injection following foam. Results showed the importance of the gas slug to subsequent liquid injectivity. However, the effects of multiple gas and liquid slugs were not explored.

In this paper, we present a coreflood study of injectivities of multiple gas and liquid slugs in a SAG process. We inject nitrogen foam, gas and surfactant solution into a sandstone core sample. The experiments are conducted at a temperature of 90°C with 40-bar back pressure. Pressure differences are measured to quantify the injectivity and supplemented with CT scans to relate water saturation to mobility.

We find that during prolonged gas injection in the first gas slug following foam, a collapsed-foam region forms near the inlet due to the interplay of evaporation, capillary pressure and pressure-driven flow. This region slowly propagates downstream. During subsequent liquid injection, liquid mobility is much greater in the collapsed-foam region than downstream, and liquid sweeps the entire core cross section there rather than a single finger. In the region beyond the collapsed-foam region, liquid fingers through foam. Liquid flow converges from the entire cross section to the finger through the region of trapped gas.

During injection of the second gas slug, the liquid finger disappears quickly as gas flows in, and strong foam forms from the very beginning. A collapsed-foam region then forms near the inlet and slowly propagates downstream with a propagation velocity and mobility similar to that in the first gas slug. Behavior of the second liquid slug is likewise similar to that of the first liquid slug.

Our results suggest that, in radial flow, the small region of foam collapse very near the well is crucial to injectivity because of its high mobility. The subsequent gas and liquid slugs behave like the first slugs. The behavior of the first gas slug and subsequent liquid slug is thus representative of near-well behavior in a SAG process.

Introduction

Foam, a dispersion of gas in a liquid phase, is widely used in a number of industries, including petroleum production (Schramm 1994) and environmental remediation (Wang and Mulligan 2004; Atteia et al. 2013). Foam is applied as an enhanced oil recovery (EOR) technique because of its capability of reducing gas mobility, improving gas-to-liquid mobility ratio, and in turn increasing gas sweep efficiency (Schramm 1994, Rossen 1996, Lake et al. 2014). Foam is also used to recover dense non-aqueous phase liquid (DNAPL) in soils in a manner similar to an EOR process (Hirasaki et al., 1997).

Foam can be placed into a reservoir by co-injecting gas and liquid (Rossen et al. 2010) or by a SAG (surfactant-alternating-gas) process, where gas slugs and surfactant-solution slugs are injected alternatively (Kibodeaux and Rossen 1997; Farajzadeh et al., 2009). SAG is usually a favored method for injecting foam, due to the excellent injectivity during gas injection (Matthews 1989, Heller 1994, Shan and Rossen 2004), as well as its ability to reduce corrosion in pipes and facilities (Matthews, 1989; Heller, 1994). However, liquid injectivity can be problematic in SAG, and fracturing of the injection well can happen during liquid injection (Kuehne et al. 1990, Martinsen and Vassenden 1999).

Injectivity is thus a crucial factor for success of a SAG process. In our previous studies, we examined liquid injectivity directly following foam by conducting core-flood experiments in Berea cores (Gong et al. 2018b). Liquid flows through foam in one or two fingers, leaving the rest foam trapped in place. Gas within and surrounding the liquid fingers dissolves into unsaturated liquid over time. This is consistent with findings in earlier core-flood studies (Kibodeaux et al. 1994, Nguyen, et al. 2009). We also reported in that study gas injectivity after foam and the liquid injectivity after a prolonged period of gas injection following foam. The experimental results suggest that the gas-slug injection has major impacts on the subsequent liquid injectivity. A collapsed-foam region forms near an injection well during gas injection and slowly propagates further from the well as more gas is injected. This region is crucial to subsequent liquid injectivity, since liquid mobility in this region during liquid injection is much greater than that further from the injection well. Based on these experimental findings, we proposed a bank-propagation model reflecting the effects of gas injection on the subsequent liquid injectivity (Gong et al. 2018a), which is not currently represented in conventional foam simulators.

Multiple gas and liquid slugs are injected in a SAG process. However, the effects of multiple gas and liquid slugs are still not clear: specifically the effects of the earlier slugs on the injectivity of later slugs. In this paper, we present a coreflood study of gas and liquid injectivities in a field core. The main goal is to examine the flow behavior during injection of multiple gas and liquid slugs in a SAG process. We also examine liquid injectivity directly following foam and after a prolonged period of gas injection following foam, in order to investigate whether the flow behavior observed in our previous studies also appears in this low-permeability field core.

Materials & Methods

Materials. A nearly homogeneous sandstone field core (Kamarul Bahrim et al. 2017) is used in these experiments. The core has a diameter of 3.8 cm and a length of 6.9 cm. A field core is typically short, though it is possible to butt short cores to make a longer composite core. We do not combine cores for a foam study, because of the experimental artefacts included by capillary end effect at each core boundary. The average porosity of the core is about 0.21, and the permeability is about 63 md.

A synthetic brine containing five salts [sodium chloride (1.84 wt%), sodium sulphate (0.28 wt%), magnesium chloride (0.73 wt%), calcium chloride (0.1 wt%) and potassium chloride (0.05 wt%)] is used to prepare surfactant solutions. The brine contains 3 wt% salinity. Surfactant A (Kamarul Bahrim et al. 2017) is used to conduct the foam experiments. The surfactant solution is at a concentration of 0.5 wt%. Nitrogen with a purity of 99.98% is the gas phase in the foam.

Experimental setup. The setup used to perform the core-flood experiments is schematically shown in Fig. 1. The core is coated with epoxy and fitted into a PEEK (polyether ether ketone) core holder, which is suitable for CT scanning because of its low X-ray attenuation. The core holder is fixed horizontally, and coated with a thermal jacket, with silicon oil flowing inside, in order to maintain the

core temperature at approximately 90°C. Two differential-pressure transducers and two absolute-pressure transducers are applied to measure the absolute pressures at positions starting from the inlet to the outlet of the core, as well as the pressure drops across the entire core (ΔP_t) and across the middle section of the core (ΔP_2). In this work, we study the middle section (Section 2), which has a length of 4.2 cm, to avoid the entrance region and the capillary-end effect. A Quizix pump is used to inject surfactant solution and control the liquid injection rate. Nitrogen is supplied from a 220-bar cylinder, and injected to the core through a mass-flow controller. A back-pressure regulator is connected to the outlet of the core holder to maintain the back pressure as 40 bar. A confining pressure, equal to the injection pressure, is applied.

A third-generation medical CT scanner (Siemens Somatom) is used to monitor water-saturation changes, and relate the water saturations to the mobilities measured in the experiments. The CT scanner is operated with single energy, at a voltage of 140 keV and a current of 250 mA. The entire core is scanned each time, which allows us to obtain the water-saturation profiles both at cross sections and along the core. The thickness of each cross-sectional CT slice is 6 mm. The resolution of each cross section is 521 × 521 pixels. An imaging software package ImageJ (Schindelin et al. 2012) is applied to visualize the three-dimensional CT images and perform the image analysis.

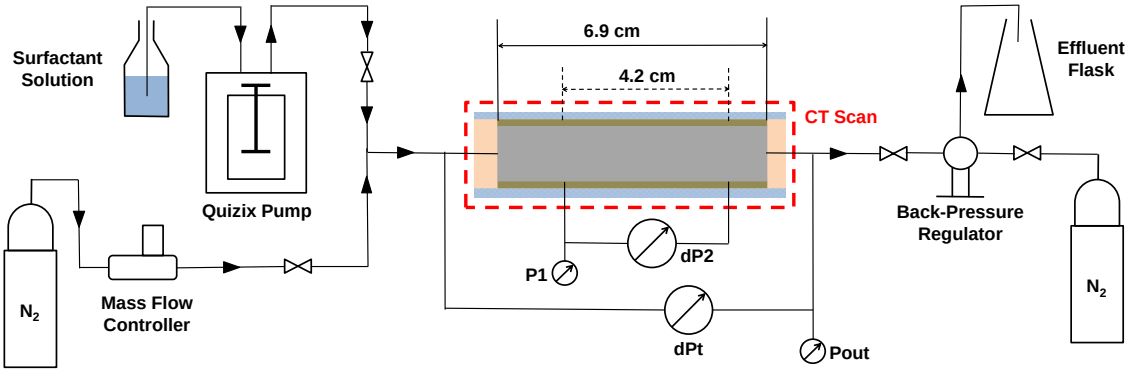

Figure 1 *Schematic of the experimental setup.*

Experimental Method. In all experiments, we first inject 0.95-quality (gas fractional flow) foam into the core by co-injecting gas (nitrogen) and surfactant solution. The total superficial velocity for foam injection is 1 ft/day. The quality 0.95 is chosen for comparison with our previous work with Berea cores (Gong et al. 2018b). In the subsequent gas- and liquid-injection periods, gas and surfactant solution are injected at superficial velocities of 6ft/day and 1ft/day, respectively.

In this study, we present three experiments (Cases A - C) in order to examine gas and liquid injectivity in different situations. First, we examine liquid injectivity directly after 0.95-quality foam (Case A). We then examine a prolonged period of gas injection after foam, and a subsequent liquid-injection period (Case B). Finally, injection of multiple large gas and liquid slugs is studied (Case C). In all experiments, there is no oil in the system. In a field application, oil may well have been displaced from the near-well region before or soon after the start of the SAG process.

Experiments & results

Since the experiments are conducted in a short field core, it is important to know whether the section studied avoids the entrance and capillary-end effects. As shown in Fig. 2, in the region of interest, the average cross-sectional water saturations during initial steady-state foam injection in Cases A – C are roughly uniform at 0.32 (Fig. 2). This suggests that the region studied is relatively free of entrance and capillary-end effects.

Case A: Liquid Injection Follows Foam. In this experiment, we inject surfactant solution directly after steady-state foam. As shown in Fig. 3, the pressure gradient evolves over three stages. In the beginning, liquid enters the core with a relatively high mobility (the initial low pressure gradient). The pressure gradient then reaches a large value, and holds constant for a period of about 2.5 PV. During this period, liquid penetrates foam in a finger, which is visible at a position 3 cm from inlet after about

3.5 PV surfactant solution is injected (Fig. 3c). The pressure gradient then decreases, reflecting displacement or dissolution of gas trapped within the finger into unsaturated injected liquid.
As presented in Figs. 3a and 3b, at a position 3 cm from inlet, the entire cross section turns from light blue to light green, indicating that the water saturation of the whole cross section increases. A liquid finger is then visible after about 3.5 PV surfactant solution is injected (Fig. 3c). The liquid finger widens as more liquid is injected (Figs. 3d-3g). Over time, the liquid finger also becomes more red, which confirms that the unsaturated liquid dissolves or displaces gas trapped within the finger. At the same time, the region outside the liquid finger turns to a deeper blue, which indicates that gas outside the finger remains trapped in place. Gas expands as absolute pressure declines, and drives down water saturation further in this region.

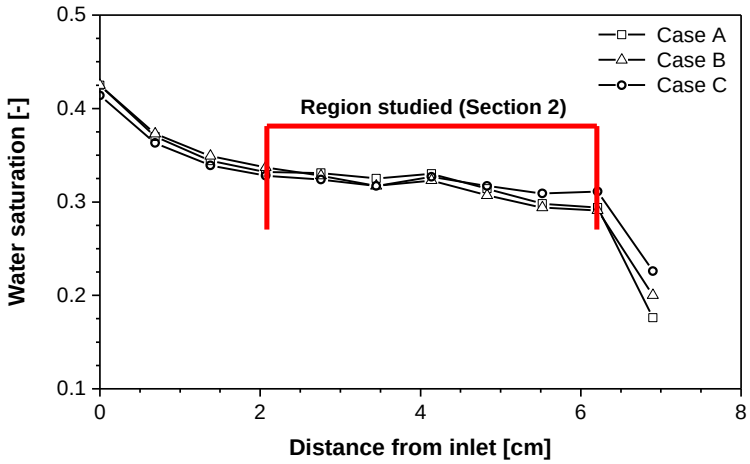

Figure 2 *Initial steady-state foam (0.95-quality) in Cases A - C.*

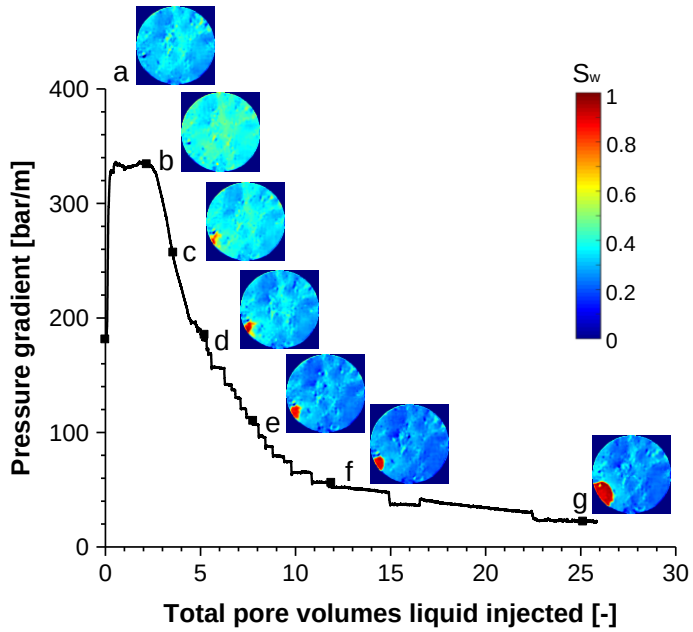

Figure 3 *Pressure gradient in section 2 during liquid injection directly following 0.95-quality foam. Images a – g show water saturation at a position 3 cm from the inlet after different periods of liquid injection: (a) initial state (steady-state foam), (b) 2.7 PV, (c) 3.5 PV, (d) 5.6 PV, (e) 7.8 PV, (f) 11.8 PV, (g) 25.3 PV.*

A quantitative analysis of the CT images in Figs. 4a, b and c supports the mechanisms proposed above. The liquid finger widens with time, so for Fig 4c we analyse a region that lies within the finger from its first appearance (Fig. 4a; cf. Fig. 3c) and a region that remains outside the finger throughout the images (Fig. 4b; cf. Fig. 3g). The average water saturation inside and outside the liquid finger both

increase from 0.3 (steady-state foam) quickly to about 0.4, and remain nearly constant until about 2.7 PV liquid injection (Fig. 4c). This suggests that ahead of the liquid finger, liquid flow disperses across the core cross section. Thereafter, a finger, with distinctly greater water saturation, appears. Water saturation inside the finger increases gradually, and finally reaches about 0.9, indicating that gas within the finger has dissolved into liquid or been displaced. This sequence suggests that gas dissolution is a key to formation of the finger, raising water relative permeability and directing liquid to flow within the finger along its length. This process is analogous to wormhole formation in acidization of carbonates, where greater flow of acid leads to greater dissolution, and in turn yet-greater flow of acid (Hoefner et al., 1987). Once the finger is evident, water saturation outside the liquid finger decreases to about 0.1 as more liquid is injected (Fig. 4c). Gas outside the liquid finger expands as pressure declines, but remains trapped at a large saturation.

In Fig. 4d, we estimate the area with distinctly higher water saturation in the cross-sectional images. As shown in Fig. 4d (cf. Figs. 3a, 3b), there is no region of distinctly greater water saturation evident in the CT-saturation image until about 2.7 PV liquid injection. The finger becomes evident as dissolution of gas within the finger greatly changes gas saturation there. The liquid finger is first evident in the CT image, occupying about 1.5% of the cross section, after about 4 PV liquid injection (cf. Fig. 3c). The finger size remains nearly unchanged for about 10 PV liquid injection (from 4 PV to 14 PV), and then grows slowly outwards as it dissolves surrounding trapped gas (cf. Figs. 3d-g).

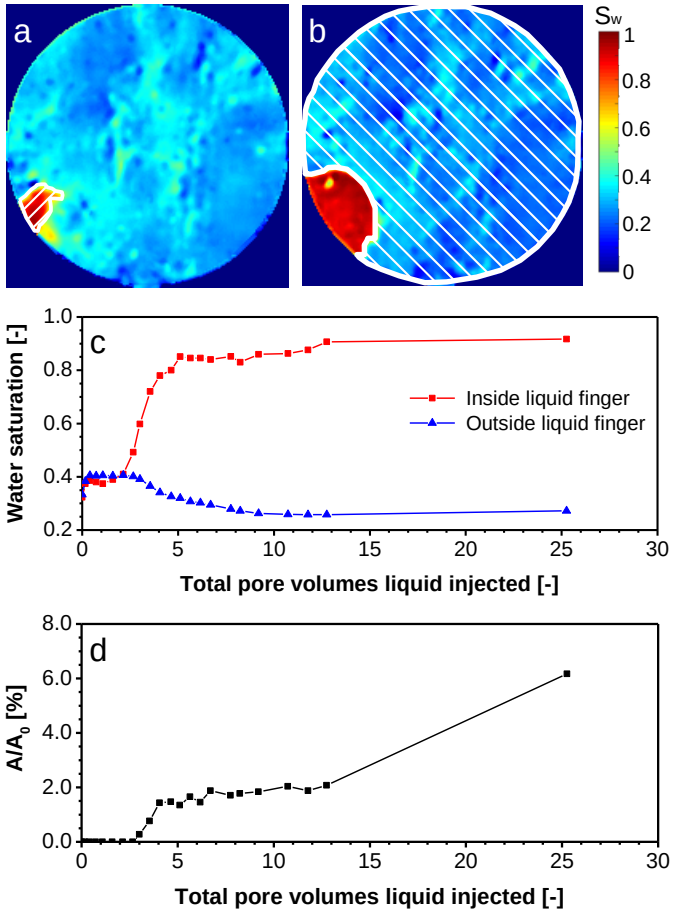

Figure 4 *Liquid finger at a position 3 cm from the inlet. (a) Region that lies inside the liquid finger (the shaded area) from its first appearance. (b) Region that lies outside the liquid finger (the shaded area) in all images. (c) Water saturation inside and outside the liquid finger. (d) Dimensionless area of the liquid finger as function of time. A is the area of the liquid finger (i.e., with S_w larger than 0.65); A_0 is the area of the entire cross section.*

Case B. Injection of Single Gas and Liquid Slugs. In this experiment, we inject surfactant solution following a prolonged period of gas injection (about 640 PV) that in turn follows steady-state foam

injection (0.95 quality). During the gas-injection period, the pressure gradient in Section 2 first decreases from 250 bar/m to a plateau value (about 50 bar/m), which lasts for about 220 PV gas injection (from about 40 PV to about 260 PV), and then experiences a second decline (Fig. 5a). The pressure gradient remains substantial in Section 2 until a large volume of gas is injected, i.e. about 470 PV. The subsequent decline in pressure gradient implies that foam greatly weakens or collapses after sufficient gas injection. This could reflect a continuous-gas foam with some gas still trapped in place (Rossen 1996).

This is confirmed by CT scans (Figs. 5b and 5c). As shown in Fig. 5b, the initial water saturation when the core is saturated with 0.95-quality foam is about 0.35 (the light green colour in Fig. 5c). After about 34.1 PV gas injection, the average cross-section water saturation decreases to about 0.25 along the whole core (the light blue colour in Fig. 5c), which indicates that gas first flushes the whole core, which makes foam in the entire core weaker. Water saturation then decreases in a wave moving downstream, i.e. from the positions 1.8 cm to 5.4 cm from the inlet (Fig. 5b), which indicates that a region of collapsed or greatly weakened foam propagates from the inlet slowly to the outlet of the core. The propagation of the collapsed-foam region can be seen in Fig. 5c: a dark blue region (marked by a yellow arrow) propagates toward the outlet (right side) as more gas is injected. After about 640 PV gas injection, the collapsed-foam region reaches the end of the core.

Thus, during a period of gas injection, gas first weakens foam (the plateau in pressure gradient). Foam collapses or greatly weakens (the second decline in pressure gradient) when a sufficient volume of gas is injected. The collapsed-foam region moves as a front from the inlet to the outlet as more gas is injected. The interplay of pressure-gradient-driven flow, evaporation of water, and capillary effects leads to foam weakening and collapse (Gong et al. 2018b).

This result is similar to that in our previous study (Gong et al. 2018a), in that prolonged gas injection leads to a collapsed-foam region that slowly propagates from the core face downstream. However, the collapsed-foam region advances more slowly and with a larger total mobility (1/588, 9.9×10^{-10} m^2/Pa s) in this study than in the Berea cores (1/400, 9×10^{-10} m^2/Pa s). In the coreflood experiments with Berea cores, foam collapsed at a water saturation of about 0.2. In this case, the water saturation at the point of foam collapse is about 0.1, as measured in the CT images. That is, the rise in mobility happens when water saturation falls to about 0.1; water saturation then continues to fall further. We believe that the water saturation after prolonged gas injection is very small, but not zero. The calculation based on CT measurements can be affected by the noise in images. For purpose of injectivity, the key event is the collapse of foam at a water saturation of about 0.1.

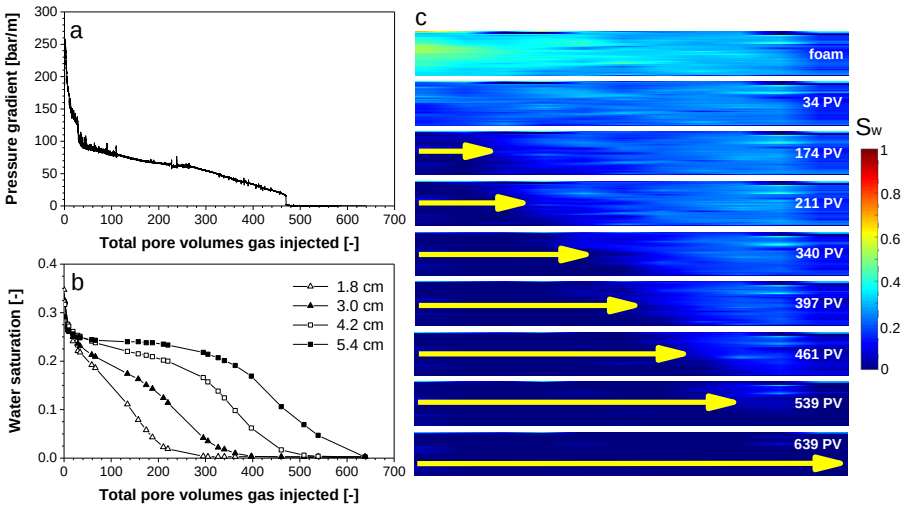

Figure 5 *Pressure gradient and water saturation during a prolonged period of gas injection following 0.95-quality foam. (a) Pressure gradient in Section 2 during gas injection following 0.95-quality foam. (b) Water saturation during gas injection in cross-sections at four different positions: 1.8 cm, 3 cm, 4.2 cm and 5.4 cm from the inlet. (c) Water-saturation profile in a vertical cross-section along the central axis of the core. The yellow arrows show the propagation of the collapsed-foam region.*

Thus, a sufficient amount of gas injection creates a collapsed-foam region propagating from the inlet of the core. This is expected to have a major impact on subsequent liquid injection. In our experiments, after about 640 PV gas injection, foam in the entire core collapses or weakens greatly, making the subsequent liquid injection 23 times easier (pressure gradient 23 times lower) than in liquid injection directly following foam (Case A). However, the pressure gradient is still 15 bar/m (not shown), which suggests that some gas remains trapped. This is confirmed by CT measurements during subsequent liquid injection (Fig. 6).

Fig. 6a shows the vertical water-saturation profile along the axis of the core during liquid injection after 640 PV gas injection, when the collapsed-foam region fills the whole core (Fig. 5c). In the beginning, the liquid front propagates from the inlet to the outlet of the core as more liquid is injected. Liquid sweeps the entire cross section without fingering (0.27 PV – 0.97 PV liquid injection in Fig. 6a). This indicates that foam collapses or greatly weakens after a prolonged period of gas injection, leaving some trapped gas, and in turn makes subsequent liquid injection much easier than following full-strength foam. After a longer period of liquid injection (8.6 PV), a high-water-saturation region appears near the bottom of the core starting at the inlet (the red region). This suggests that preferential paths for liquid flow develop within the collapsed-foam region; these can be seen more clearly in Fig. 6b. Since the mobility within this region is already high, this would be expected to make only a minor difference to injectivity.

Fig. 6b presents the water-saturation profile at a position 3 cm from the inlet over time. The cross-section is dark blue after about 0.27 PV liquid injection, since liquid has not yet arrived at this position. After about 1.9 PV liquid is injected, the whole cross section has turned to light yellow, reflecting liquid sweep of the entire cross section. Starting from 5.8 PV liquid injection, some regions turn red as more liquid is injected. This confirms that liquid finds preferential paths after about 5.8 PV liquid injection. The liquid preferential paths expand outward over time.

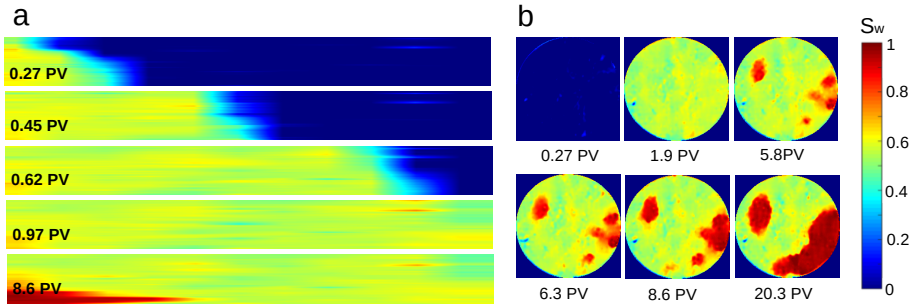

Figure 6 *Water-saturation profile during liquid-injection period after 640 PV gas injection following 0.95-quality foam. (a) Water-saturation profile in a vertical cross-section along the central axis of the core. (b) Water saturation profile at 3 cm from the inlet after different amounts of liquid injection.*

Case C. Injection of Multiple Gas and Liquid Slugs. In this experiment, we examine the injectivity of multiple gas and liquid slugs. The gas and liquid slugs are injected in the following sequence: 0.95-quality foam injection; first gas slug (about 250 PV); first liquid slug (about 26 PV); second gas slug (about 150 PV); second liquid slug (about 38 PV). The pressure gradients and the water saturation profiles during injection of the two gas slugs and the two liquid slugs are compared, respectively.

As shown in Fig. 7, overall, the two gas slugs show a similar behaviour in pressure gradient. The pressure gradients for both the first and the second gas slug quickly reach a peak and then decrease to a plateau. The peak values of pressure gradient for the two gas slugs are comparable, about 220 bar/m for the first gas slug, and about 250 bar/m for the second gas slug, which indicates that the two gas slugs quickly reach a similar state.

As mentioned above, the core is saturated with steady-state foam before injection of the first gas slug, while a period of liquid injection (the first liquid slug) precedes the second gas slug. Thus, the similarity in the peak values of the pressure gradients implies that strong foam is generated in the beginning of the injection of the second gas slug. A SAG process works well in generating foam in this case. This is confirmed by the CT measurements.

Fig. 8 shows the average water saturation of cross sections at four positions along the core, during injection of the first (Fig. 8a) and the second (Fig. 8b) gas slugs. During injection of the first gas slug,

the initial water saturation is about 0.3 for all four positions (reflecting steady-state foam). During injection of the second gas slug, water saturation starts from values larger than 0.3, since a liquid slug was injected beforehand. For the positon 1.8 cm from the inlet, the initial water saturation is about 0.65. The main reason is that the position 1.8 cm from the inlet is within the collapsed-foam region created during the first period of gas injection; the first liquid slug then sweeps the entire cross section with a high water saturation. The water saturation then quickly decreases to about 0.3 for all the positions, as gas displaces liquid in the core and foam is generated. Thereafter the water saturation for the two gas slugs follows nearly the same trend. At the position 1.8 cm from the inlet, the average cross-sectional water saturation decreases gradually to about 0.1 after about 150 PV gas injection (Figs. 8a and 8b), and to nearly zero after about 250 PV gas is injected (Fig. 8a). However, at a position further downstream, close to the outlet, i.e. 5.4 cm from the inlet, the water saturation holds nearly constant during this period. This means that foam collapses at the position 1.8 cm from the inlet, while 5.4 cm from the inlet is beyond the collapsed-foam region (Figs. 8a and 8b).

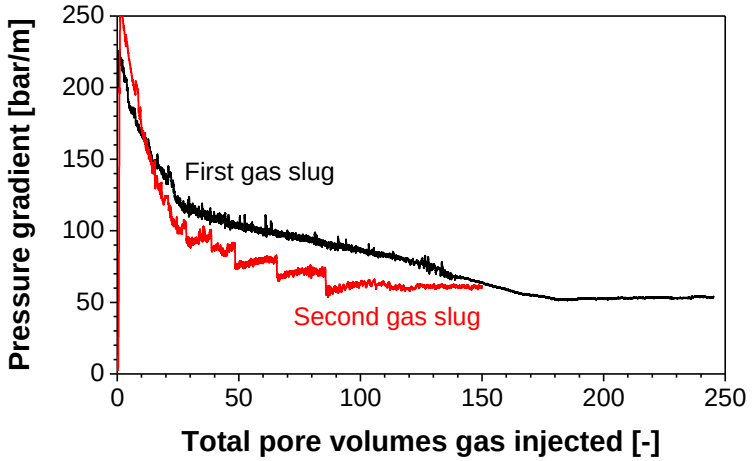

Figure 7 *Pressure gradient in Section 2 during the first and second gas slug injection in a SAG process.*

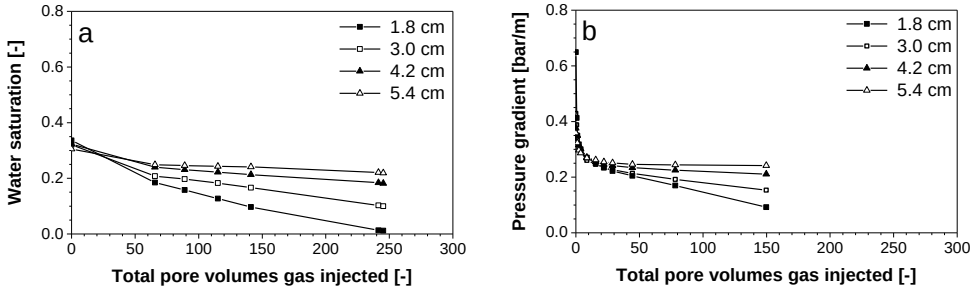

Figure 8 *Average water saturation in the entire cross section at different positions along the core during gas injection. (a) First gas slug injection. (b) Second gas slug injection.*

Fig. 9 presents the axial water-saturation profile during injection of the two gas slugs. A wide liquid finger forms near the inlet during injection of the first liquid slug (cf. Fig. 9b, top; cf. Fig. 6). The liquid finger disappears quickly as gas flows in (Fig. 9b, subsequent CT images). After about 1.2 PV gas injection in the second gas slug, the water-saturation profile becomes similar to the initial state during injection of the first gas slug (steady-state foam). This confirms that foam is generated quickly as the second gas slug is injected. As more gas is injected, the collapsed-foam region propagates downstream from the inlet. The front of the collapsed-foam region arrives at a similar position after a similar amount of gas is injected, i.e. 141 PV for the first gas slug, and 150 PV for the second gas slug (images in the bottom row of Figs. 9a and 9b). This suggests that the collapsed-foam region propagates with similar velocities during the two periods of gas injection. Thus, the second gas slug behaves like the first gas slug, both within and beyond the collapsed-foam region.

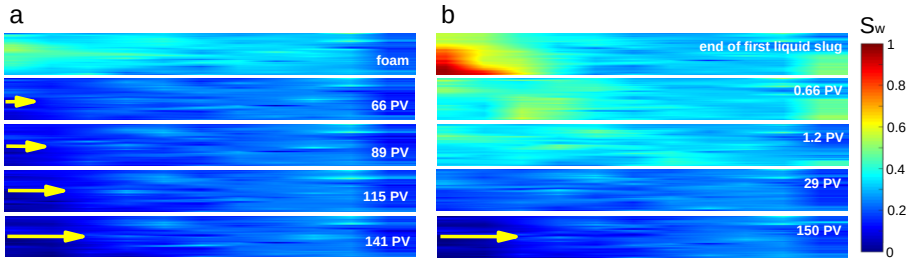

Figure 9 *Water-saturation profile in a vertical cross-section along the central axis of the core during gas-injection periods. (a) First gas slug. (b) Second gas slug.*

During the first and the second periods of liquid injection, the pressure gradient first rises to a large value, remains nearly constant for a time, and then decrease to a small value (Fig. 10). The pressure gradient in both cases has a similar shape to that for liquid injection directly following foam (Case A). However, the plateau values of the pressure gradient for the first and the second periods of liquid injection in a SAG process are smaller than the value for the case where liquid injection directly follows foam, which is about 340 bar/m (cf. Fig. 3). The plateau pressure gradient during injection of the first liquid slug is smaller than that during injection of the second liquid slug.
The reason is that a larger gas slug was injected before the first liquid slug (250 PV) than before the second liquid slug (150 PV). The larger gas slug creates a larger collapsed-foam region in the core, which in turn reduces the pressure gradient during subsequent liquid injection. This is supported by the CT measurements. As shown in Fig. 11, at the end of the injection of the first and second gas slugs, there are dark blue regions on the left side of the images for both gas slugs. The dark blue region is larger at the end of the injection of the first gas slug than at the end of the injection of the second gas slug; the collapsed-foam region is larger before the injection of the first liquid slug.
When liquid is injected, the two liquid slugs behave similarly: liquid first quickly fills the collapsed-foam region (the yellow region on the left side of the images on the second row in Fig. 11), in which there is less trapped gas. As more liquid is injected, the water saturation in the middle of the core becomes more red over time in the collapsed-foam region, while beyond the collapsed-foam region, it first turns to light green and then to light blue (Fig. 11). However, what happens in the weakened-foam region cannot be fully seen from the axial CT images, since the liquid flow path can be tortuous, moving in and out of this axial cross section. In order to understand the flow behaviour in the weakened-foam region during the two liquid-injection periods, we study the cross-sectional water saturation profiles perpendicular to the axis of the core (Figs. 12 and 13).

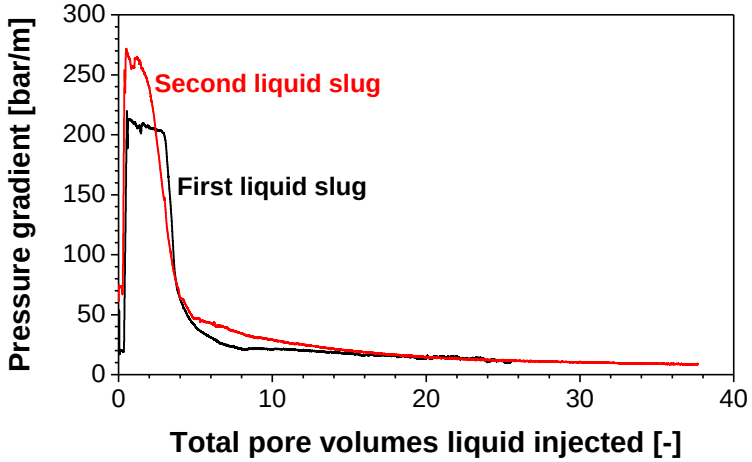

Figure 10 *Pressure gradient in Section 2 during injection of the first and second liquid slugs in a SAG process.*

Fig. 12 shows the average water saturation in cross sections during the injection of the first liquid slug. As presented in Fig. 12a, at the end of the injection of the first gas slug, the core is occupied by two banks, the collapsed-foam bank and the weakened-foam bank. The yellow line represents the

front of the collapsed-foam bank. The water saturation over time at two positions are presented, one within the collapsed-foam region (1.2 cm from the inlet, Fig. 12b), and the other beyond the collapsed-foam region (3 cm from inlet, Fig. 12c). In the collapsed-foam region, liquid first flushes the entire cross section, and then forms preferential paths after a period of liquid injection, i.e. 2.5 PV in this case (Fig. 12b). In the weakened-foam region, liquid does not sweep the entire cross section. Liquid fingers through foam as in liquid injection directly following foam (Fig. 12c). The liquid finger is visible after about 2.5 PV surfactant solution is injected.

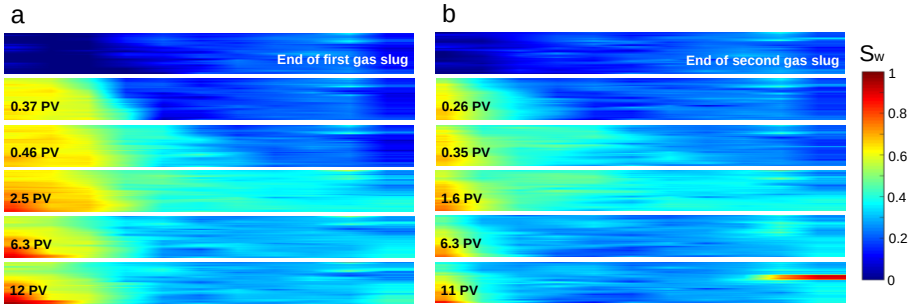

Figure 11 *Water-saturation profile in a vertical cross-section along the central axis of the core during liquid injection. (a) First liquid slug. (b) Second liquid slug.*

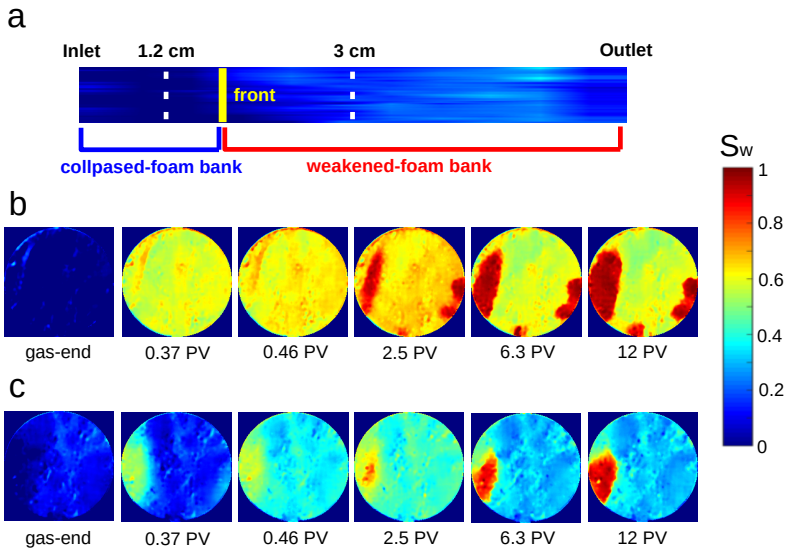

Figure 12 *Water-saturation profile during the first liquid slug injection. (a) Axial vertical cross-section showing collapsed-foam bank and weakened-foam bank created before injection of the first liquid slug. (b) Water-saturation profile at a position within the collapsed-foam bank (1.2 cm from inlet) after different amounts of liquid injection. (c) Water-saturation profile at a position beyond the collapsed-foam bank (3 cm from inlet) after different amounts of liquid injection.*

Fig. 13 presents water saturation at the same two positions along the core during injection of the second liquid slug. Similar to the first liquid slug, liquid first quickly flows through the collapsed-foam region with high mobility, and then fingers through trapped gas beyond the collapsed-foam region.

In general, foam in this relatively-low-permeability field core behaves similarly to its behaviour in the Berea cores (Gong et al. 2018b) during liquid injection after a period of gas injection following foam. Liquid first quickly fills the collapsed-foam region, then fingers through the weakened-foam region. Gas within and surrounding the liquid fingers dissolves or is displaced over time. However, compared to the results with the Berea cores (Gong et al. 2018a), in this case, the liquid-fingering bank propagates with a slower dimensionless velocity with a lower total mobility (1.4, 1.4×10^{-13} m^2/Pa s). The gas-dissolution bank propagates with a greater dimensionless velocity, and a lower total mobility (0.2, 2×10^{-12} m^2/Pa s). The corresponding values for the Berea cores were 3.3 (dimensionless velocity)

and 8.5×10^{-13} m^2/Pa s (total mobility) for the liquid-fingering bank; 0.08 (dimensionless velocity) and 6.6×10^{-11} m^2/Pa s (total mobility) for the gas-dissolution bank (Gong et al. 2018a).

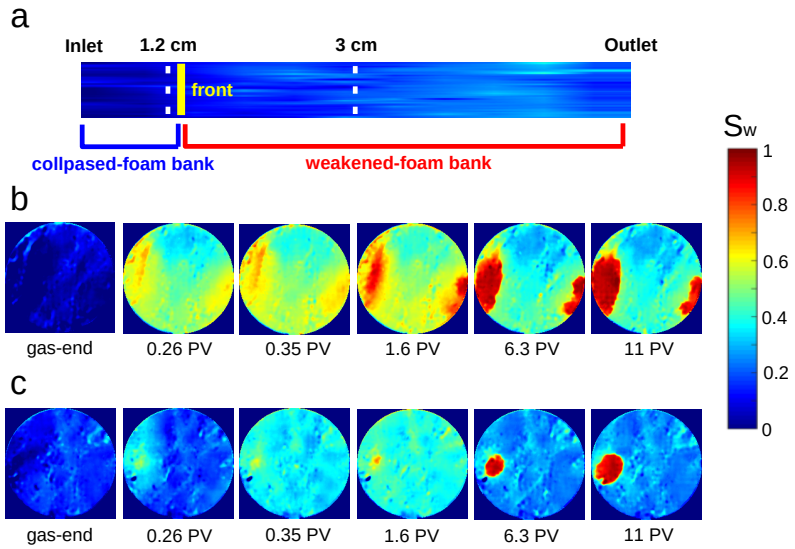

Figure 13 *Water-saturation profile during injection of the second liquid slug. (a) collapsed-foam bank and weakened-foam bank created before injection of the first liquid slug. (b) Water-saturation profile at a position within the collapsed-foam bank (1.2 cm from inlet) after different amounts of liquid injection. (c) Water-saturation profile at a position beyond the collapsed-foam bank (3 cm from inlet) after different amounts of liquid injection.*

Fig. 14 compares the properties of the liquid finger at the same position (3 cm from the inlet, beyond the collapsed-foam region) during the two periods of liquid injection. In general, the second liquid slug behaves like the first liquid slug. The initial water saturation outside the liquid finger is also about 0.2. Similar to what we observed in liquid injection directly following foam (Case A), the average water saturation outside the liquid finger first quickly reaches a plateau at about 0.45, which lasts about 2.5 PV, and then decreases to about 0.25 - 0.3 over time (Fig. 14a). Unlike liquid injection directly following foam (Case A), the average water saturation inside the liquid finger increases from about 0.2 (after a period of gas injection) to about 0.9 within a slort time. In contrast, water saturation outside the finger holds steady (cf. Fig. 4). One possible reason is that a period of gas injection weakens foam, making it easier for liquid to form a finger. Figs. 12 and 13 show that the liquid fingers become visible more quickly (within 1 PV liquid injection) than with liuqid injection direction following foam. The liquid finger grows outwards as more liquid is injected for both liquid slugs, although the liquid finger formed during injection of the second liquid slug is smaller than that formed during injection of the first liquid slug (Fig. 14b).

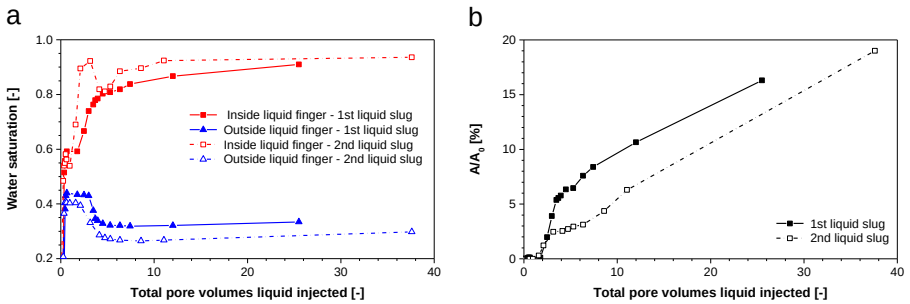

Figure 14 *Liquid finger visible at 3 cm from inlet. (a) Water saturation inside and outside the liquid finger during the injection of the first and second liquid slugs. (b) Dimensionless area of the liquid finger during the injection of the first and second liquid slugs. A is the area of the liquid finger (S_w larger than 0.65); A_0 is the total area of the cross section.*

Concluding Remarks

In this work, we examine liquid and gas injectivity in different situations. We present the first core-flood study of the mobilities and the propagation of banks during the injection of multiple large gas and liquid slugs in a SAG-foam process.

Liquid injectivity directly following foam is very poor, as shown in previous studies. Liquid first sweeps the entire core cross section, then penetrates trapped foam in a finger, with greater water saturation. Gas dissolution is the key for forming the liquid finger and directing liquid to flow through the finger. Thereafter, liquid flows only or primarily through the finger. Within the liquid finger, gas dissolves into unsaturated liquid that flows through the finger; some gas displacement within the finger is also possible. Little liquid flows outside the liquid finger; gas remains trapped there. The liquid finger grows outward over time, as gas surrounding the finger dissolves into injected liquid. During a prolonged period of gas injection following foam, gas first weakens foam in the entire core. Then a collapsed-foam region, in which gas mobility is much greater, forms near the inlet and propagates slowly downstream. During subsequent liquid injection, liquid sweeps the entire core cross section in the collapsed-foam region, while liquid fingers through the weakened-foam region.

In a SAG process, the second gas and liquid slugs show similar behavior to the first gas and liquid slugs. Although a wide liquid finger forms during injection of the first liquid slug, it disappears quickly when the injection of the second gas slugs begins. The peak value of the pressure gradient during the second period of gas injection is comparable to that for steady-state foam before the injection of the first gas slug. Clearly, a SAG process forms strong foam in this case. In the two gas-injection periods, a collapsed-foam region propagates downstream with similar propagation velocities and similar mobilities. During the two subsequent liquid-injection periods, liquid fills the collapsed-foam region, and fingers through the weakened-foam region with similar propagation velocities and mobilities. The behavior of the first gas and liquid slug extends to the subsequent slugs. In other words, the behavior of the first gas and liquid slugs is representative of gas and liquid injectivity in a SAG process.

In our previous work (Gong et al., 2018a), we show the implications of the behavior like that seen in this study for injectivity in SAG processes. This work shows that the model could be applied to the near-well region in a SAG process with multiple slugs. Current foam models do not represent fine-scale liquid fingering and capillary trapping of gas in foam well, and extraordinary grid refinement would be needed to represent a collapsed-foam region propagating slowly from an injection well. Nonetheless, these effects have major impacts on the subsequent liquid injectivity.

Acknowledgement

Authors thank PETRONAS and Shell Global Solutions International B.V. for supporting our work and permission to publish this work. We thank Steffen Berg for help with image analysis strategies. We also thank Michiel Slob and Ellen de Koning for their help with the experiments.

Reference

Atteia, O., Estrada, E. D. C., Bertin, H.[2013] Soil Flushing: A Review of the Origin of Efficiency Variability. *Reviews in Environmental Science and Bio/Technology*, **12**(4), 379–389.

Farajzadeh, R., Andrianov, A, Zitha, P. L. J. [2009] Investigation of Immiscible and Miscible Foam for Enhancing Oil Recovery. *Industrial & Engineering chemistry research* **49** (4), 1910-1919

Gong, J., Vincent Bonnieu, S., Kamarul Bahrim, R. Z., Che Mamat, C. A. N. B., Tewari, R.D., Groenenboom, J., Farajzadeh, R., Rossen, W.R. [2018] Modelling of Liquid Injectivity in Surfactant-Alternating-Gas Foam Enhanced Oil Recovery. *Accepted for publication by SPE Journal*. SPE-190435-PA.

Gong, J., Vincent Bonnieu, S., Kamarul Bahrim, R. Z., Che Mamat, C. A. N. B., Groenenboom, J., Farajzadeh, R., Rossen, W.R. [2018] Laboratory Investigation of Liquid Injectivity in Surfactant-Alternating-Gas Foam Enhanced Oil Recovery. *Accepted for publication by Transport in Porous Media*.

Heller, J. P. [1994] *CO2 Foams in Enhanced Oil Recovery*. In: Schramm, L. L. Foams: Fundamentals and Applications in the Petroleum Industry, pp. 201-234. American Chemical Society, Washington, D.C.

Hirasaki, G., Miller, C. A., Szafranski, R., Tanzil, D., Lawson, J. B., Meinardus, H., Jin, M., Londergan, J. T., Pope, G. A. [1997] Field Demonstration of the Surfactant/Foam Process for Aquifer Remediation. *SPE Annual Technical Conference and Exhibition*, San Antonio, Texas, USA.

Hoefner, M. L., Fogler, H S., Stenius, P., and Sjoblom, J. [1987] Role of Acid Diffusion in Matrix Acidizing of Carbonates. *Journal of Petroleum Technology*, **39**(02), 203-208.

Kamarul Bahrim, R. Z., Zeng, Y., Vincen Bonnieu, S., Groenenboom, J., Tewari, R. D., and Biswal, S. L. [2017] A Study of Methane Foam in Reservoir Rocks for Mobility Control at High Temperature with Varied Permeabilities: Experiment and Simulation. *SPE/IATMI Asia Pacific Oil & Gas Conference and Exhibition*, Jakarta, Indonesia

Kuehne, D. L., Ehman, D. I., Emanuel, A. S., Magnani, C. F. [1990] Design and Evaluation of a Nitrogen-Foam Field Trial. *Journal of Petroleum Technology*, **42**(02), 504 – 512.

Kibodeaux, K. R., Zeilinger, S. C., Rossen, W. R. [1994] Sensitivity Study of Foam Diversion Processes for Matrix Acidization. *SPE Annual Technical Conference and Exhibition*, New Orleans, Louisiana, USA.

Kibodeaux, K. R., Rossen, W. R. [1997] Coreflood Study of Surfactant-Alternating-Gas Foam Processes: Implications for Field Design. *SPE Western Regional Meeting*, Long Beach, California, USA.

Lake, L. W., Johns, R. T., Rossen, W. R., Pope, G. A. [2014] *Fundamentals of Enhanced Oil Recovery*. Society of Petroleum Engineers, Richardson, TX.

Matthews, C. S. [1989] Carbon Dioxide Flooding. In: Donaldson, E. C., Chilingarian, G. V., Yen, T. F. (eds.) Developments in Petroleum Science, pp. 129-156. Elsevier, Amsterdam.

Martinsen, H. A. and Vassenden, F. [1999] Foam-Assisted Water Alternating Gas (FAWAG) Process on Snorre. *European IOR Symposium*, Brighton, UK.

Nguyen, Q. P., Zitha, P. L. J., Currie, P. K., Rossen, W. R. [2009] CT Study of Liquid Diversion with Foam. *SPE Production & Operations*, **24**(01), 12 – 21.

Rossen, W. R. [1996] *Foams in Enhanced Oil Recovery*. In: Prud'homme, R.K., Khan, S.A. (eds.) Foams: Theory, Measurements and Applications, pp. 413 – 464. Marcel Dekker, New York City.

Rossen, W. R., van Duijn, C. J., Nguyen, Q. P., Shen, C., Vikingstad, A. K. [2010] Injection Strategies to Overcome Gravity Segregation in Simultaneous Gas and Water Injection into Homogeneous Reservoirs. *SPE Journal*, **15**(01), 76 – 90.

Schramm, L. L. [1994] *Foams: Fundamentals and Applications in the Petroleum Industry*. American Chemical Society, Washington, D.C.

Shan, D., Rossen, W. R.[2004] Optimal Injection Strategies for Foam IOR. *SPE Journal*, **9**(02), 132 – 150.

Schindelin, J., Arganda-Carreras, I., Frise, E., Kaynig, V., Longair, M., Pietzsch, T., Preibisch, S., Rueden, C., Saalfeld, S., Schmid, B., Tinevez, J. Y., White, D. J, Hartenstein, V., Eliceiri, K., Tomancak, P., Cardona, A. [2012] Fiji: An Open-Source Platform for Biological-Image Analysis. *Nature methods*, **9**(7): 676-682.

Wang, S., Mulligan, C. N. [2004] An Evaluation of Surfactant Foam Technology in Remediation of Contaminated Soil. *Chemosphere*, **57**(9), 1079–1089.